Distinct Interactions of 2'- and 3'–(-Methyl)anthraniloyl-Isomers of ATP and GTP with the Adenylyl Cyclase Toxin of , Edema Factor

Srividya Suryanarayana, Jenna L. Wang, Mark Richter, Yuequan Shen, Wei-Jen Tang, Gerald H. Lushington, Roland Seifert

Accepted Manuscript

Title: Distinct Interactions of 2′- and 3′-*O*-(*N*-Methyl)anthraniloyl-Isomers of ATP and GTP with the Adenylyl Cyclase Toxin of *Bacillus anthracis*, Edema Factor

Authors: Srividya Suryanarayana, Jenna L. Wang, Mark Richter, Yuequan Shen, Wei-Jen Tang, Gerald H. Lushington, Roland Seifert

PII: S0006-2952(09)00264-0
DOI: doi:10.1016/j.bcp.2009.04.006
Reference: BCP 10142

To appear in: *BCP*

Received date: 18-2-2009
Revised date: 26-3-2009
Accepted date: 6-4-2009

Please cite this article as: Suryanarayana S, Wang JL, Richter M, Shen Y, Tang W-J, Lushington GH, Seifert R, Distinct Interactions of 2′- and 3′-*O*-(*N*-Methyl)anthraniloyl-Isomers of ATP and GTP with the Adenylyl Cyclase Toxin of *Bacillus anthracis*, Edema Factor, *Biochemical Pharmacology* (2008), doi:10.1016/j.bcp.2009.04.006

Distinct Interactions of 2'- and 3'-*O*-(*N*-Methyl)anthraniloyl-Isomers of ATP and GTP with the Adenylyl Cyclase Toxin of *Bacillus anthracis*, Edema Factor

Srividya Suryanarayana[a,+], Jenna L. Wang[b], Mark Richter[a], Yuequan Shen[c], Wei-Jen Tang[d], Gerald H. Lushington[b] and Roland Seifert[e,*]

[a]Department of Molecular Biosciences, The University of Kansas, Lawrence, KS 66045, USA

[b]Molecular Graphics and Modeling Laboratory, The University of Kansas, Lawrence, KS 66045, USA

[c]College of Life Sciences, Nankai University, 300071 Tianjin, People's Republic of China

[d]Ben May Department or Cancer Research, The University of Chicago, Chicago, IL 60637, USA

[e]Department of Pharmacology, Hannover Medical School, Carl-Neuberg-Str. 1, D-30625 Hannover, Germany

[+]present address: Department of Microbiology and Molecular Genetics, Medical College of Wisconsin, Milwaukee, WI 53226, USA

*Corresponding author. Tel.: +49 511 532 2805; fax: +49 511 532 4081; email address: seifert.roland@mh-hannover.de

Classification: Antibiotics and Chemotherapeutics

Abbreviations: AC, adenylyl cyclase; EF3, catalytic domain of edema factor adenylyl cyclase; CaM, calmodulin; EF, full-length edema factor adenylyl cyclase toxin; FRET, fluorescence resonance energy transfer; MANT, *N*-(methyl)anthraniloyl.

Abstract

Anthrax disease is caused by the spore-forming bacterium, *Bacillus anthracis*. *Bacillus anthracis* produces a calmodulin-activated adenylyl cyclase (AC) toxin, edema factor (EF). Through excessive cAMP accumulation EF disrupts host defence. In a recent study (Taha et al., Mol Pharmacol 2009;75:693-703) we showed that various 2'(3')-*O*-*N*-(methyl)anthraniloyl (MANT)-substituted nucleoside 5'-triphosphates are potent inhibitors (K_i values in the 0.1-5 μM range) of purified EF. Upon interaction with calmodulin we observed efficient fluorescence resonance energy transfer (FRET) between tryptophan and tyrosine residues of EF and the MANT-group of MANT-ATP. Molecular modelling suggested that both the 2'- and 3'-MANT-isomers can bind to EF. The aim of the present study was to examine the effects of defined 2'- and 3'-MANT-isomers of ATP and GTP on EF. 3'-MANT-2'-deoxy-ATP inhibited EF more potently than 2'-MANT-3'-deoxy-ATP, whereas the opposite was the case for the corresponding GTP analogs. Calmodulin-dependent direct MANT-fluorescence and FRET was much larger with 2'-MANT-3'-deoxy-ATP and 2'-MANT-3'-deoxy-GTP compared to the corresponding 3'-MANT-2'-deoxy-isomers and the 2'(3')-racemates. K_i values of MANT-nucleotides for inhibition of catalysis correlated with K_d values of MANT-nucleotides in FRET studies. Molecular modelling indicated different positioning of the MANT-group in 2'-MANT-3'-deoxy-ATP/GTP and 3'-MANT-2'-deoxy-ATP/GTP bound to EF. Collectively, EF interacts differentially with 2'-MANT- and 3'-MANT-isomers of ATP and GTP, indicative for conformational flexibility of the catalytic site and offering a novel approach for the development of potent and selective EF inhibitors. Moreover, our present study may serve as a general model of how to use MANT-nucleotide isomers for the analysis of the molecular mechanisms of nucleotide/protein interactions.

Key words: edema factor, calmodulin, MANT-nucleotide, fluorescence spectroscopy, molecular modelling

1. Introduction

Anthrax disease is caused by the spore-forming bacterium, *Bacillus anthracis* [1]. *Bacillus anthracis* produces an AC toxin, referred to as EF. ACs catalyze the conversion of ATP into cAMP and PP_i. Following translocation of EF into host cells by the helper toxin, protective antigen, EF is then activated by CaM [2,3]. CaM-activated EF exhibits an extremely high catalytic activity, resulting in massive cAMP formation and hence, disruption of host defence. While antibiotic treatment is effective against multiplication of bacteria, antibiotics are ineffective against toxemia. Thus, effective EF inhibitors would provide a most valuable complementation of anthrax treatment [4,5].

As an important step towards the achievement of this ambitious goal, we have resolved the crystal structure of several nucleotide-EF-CaM complexes and characterized the amino acids responsible for substrate binding and catalysis [2-4]. Additionally, we identified 2'(3')-*O*-ribosyl-substituted MANT-nucleotides as potent inhibitors of mammalian ACs and EF [5-9]. Intriguingly, mammalian ACs and EF are differentially inhibited by various MANT-nucleotides, indicating that the development of potent and selective EF inhibitors is feasible. Moreover, MANT-nucleotides are environmentally sensitive fluorescent probes [10], rendering it possible to monitor activation-dependent conformational changes in ACs [5,8,9].

Molecular modelling studies indicated that MANT-nucleotides can bind to the catalytic site of EF both as 2'-*O*-ribosyl- and 3'-*O*-ribosyl isomer [5]. Unfortunately, in 2'(3')-*O*-ribosyl-substituted MANT-nucleotides, the MANT-group isomerizes spontaneously between the 2'- and 3'-position [10], rendering it impossible by enzymatic and fluorescence spectroscopy methods to determine which isomer is preferred for binding to the catalytic site [5]. Fig. 1 shows the structures of MANT-ATP and MANT-GTP. Until recently, the analysis of the question of isomer-preference of EF was only possible by means of crystallographic approaches since 2'-MANT-3'-deoxy- and 3'-MANT-2'-deoxy isomer pairs of ATP and GTP were not commercially available [8,9]. In these compounds, isomerisation is not anymore

possible because the second crucial hydroxyl group at the ribosyl moiety of nucleotides is missing (Fig. 1) [10]. When we started the MANT-nucleotide isomer project in 2004, we had to obtain 2'-MANT-3'-deoxy-GTP as very expensive custom synthesis product. Fortunately, the 2'-MANT-3'-deoxy- and 3'-MANT-2'-deoxy isomer pairs of ATP and GTP are now commercially available to the scientific community as regular catalog products (see Materials and Methods).

Having in hands two pairs of MANT-nucleotide isomers and the respective racemic MANT-nucleotides, we could assess, for the first time, the important question which impact 2'- and 3'-*O*-ribosyl substitution has on interaction of MANT-nucleotides with ACs, specifically EF, using enzymatic and fluorescence spectroscopy approaches. The major aim of the present study was actually not to develop potent and selective EF inhibitors but rather to use EF as a general model for the interaction of proteins with MANT-nucleotide isomers because EF is a well-characterized target protein that can be obtained in large amounts for biochemical and biophysical studies. The approach used in the present study can be readily applied to any other target protein that binds MANT-nucleotides [10].

2. Materials and Methods

2.1. Materials. MANT-ATP, 2'-MANT-3'-deoxy-ATP, 3'-MANT-2'-deoxy-ATP, MANT-GTP, 2'-MANT-3'-deoxy-GTP and 3'-MANT-2'-deoxy-GTP were obtained from Jena Bioscience (Jena, Germany). [α-^{32}P]ATP (3,000 Ci/mmol) was purchased from PerkinElmer (Boston, MA, USA). EF3 was purified as described [3]. Sources of all other materials were as described before [5-9].

2.2 AC activity assay. AC activity was determined as described [5]. Briefly, assay tubes contained 10 µl of MANT-nucleotides at final concentrations from 1 nM to 100 µM as

appropriate to obtain saturated inhibition curves and 20 µl of EF3 (10 pM final concentration) in 75 mM Tris/HCl, pH 7.4, containing 0.1% (mass/vol) bovine serum albumin. Tubes were preincubated for 2 min at 25°C, and reactions were initiated by the addition of 20 µl of reaction mixture consisting of the following components to yield the given final concentrations; 100 mM KCl, 100 µM free Ca^{2+}, 5 mM free Mn^{2+} or Mg^{2+}, 100 µM EGTA, 100 µM cAMP, 100 nM CaM. ATP was added as non-labeled substrate at a final concentration of 40 µM and as radioactive tracer [α-^{32}P]ATP (0.2 µCi/tube). Tubes were incubated for 10 min at 25°C, and reactions were stopped by the addition of 20 µL of 2.2 N HCl. Denaturated protein was sedimented by a 1-min centrifugation at 13,000 x g. [^{32}P]cAMP was separated from [α-^{32}P]ATP by transferring the samples to columns containing 1.4 g of neutral alumina. [^{32}P]cAMP was eluted by the addition of 4 ml of 0.1 M ammonium acetate solution, pH 7.0. Blank values were about 0.02% of the total amount of [α-^{32}P]ATP added; substrate turnover was <3% of the total amount of [α-^{32}P]ATP added. Samples collected in scintillation vials were filled up with 10 ml of double-distilled water and Čerenkov radiation was measured in a PerkinElmer Tricarb 2800TR liquid scintillation counter. K_i values reported in Table 1 were calculated using the Prism 4.02 software (Graphpad, San Diego, CA) based on published K_m values [5,6].

2.3. Fluorescence experiments for monitoring MANT-nucleotide binding to EF.

Fluorescence experiments were performed as described [5,8,9] using quartz UV ultra-microcuvettes from Hellma (Müllheim, Germany, type 105.250-QS, light path length 10 x 2 mm, center 15 mm, total volume 150 µl) in a thermostated multicell holder at 25°C in a Varian Cary Eclipse fluorescence spectrometer (Varian, Walnut Creek, CA, USA). Cuvettes contained 140 µl of buffer consisting of 100 mM KCl, 100 µM $CaCl_2$, 10 mM $MnCl_2$ and 25 mM HEPES/NaOH, pH 7.4. Five µl of 10 µM EF3 (final concentration 300 nM), 5 µl of 10

μM CaM (final concentration 300 nM) and MANT-nucleotides (final concentration 300 nM each) were added. Steady-state fluorescence emission spectra of MANT-nucleotides in FRET experiments were recorded at low speed in the scan mode at λ_{em} 300-550 nm with λ_{ex} 280 nm. In direct fluorescence experiments, the MANT-group was excited at λ_{ex} 350 nm, and emission was recorded at λ_{em} 370-550 nm. In MANT-nucleotide saturation experiments, nucleotides were used at concentrations from 10 nM to 1.3 μM and CaM-induced FRET responses were recorded. In these experiments, MANT-nucleotide fluorescence was corrected for inner filter effect by recording the absorbance spectra of nucleotides. Those values were subtracted from the respective fluorescence recordings. Fluorescence recordings were analyzed with the spectrum package of the Varian Cary Eclipse software version 1.1.

2.4. Molecular modeling. A model for the EF receptor was constructed from the crystal structure of EF in complex with CaM and the inhibitor, 3'-deoxy-ATP [2]. Residues with no atoms within 12 Å of the co-crystallized inhibitor were truncated from the model, and all heteroatoms except the *in situ* Mn^{2+} were omitted. The remaining structure was protonated in SYBYL [12] according to standard amino acid valences at biological pH. Atomic electrostatics were modeled *via* the Gasteiger-Marsili charge formalism [13] as implemented in SYBYL, with all atoms left at their default formal charge settings except the *in situ* Mn^{2+}. All ligands were sketched and protonated in SYBYL, and Gasteiger-Marsili charges were assigned, again according to the version implemented in SYBYL. In each ligand, all oxygen atoms on terminal phosphates were considered as unprotonated, with one O atom assumed to be sp^2-hybridized (formal charge of zero) and the other two O atoms were assumed to be fully sp^3-hybridized (formal charge of -1 each). On non-terminal phosphate groups, both O atoms were assumed to resonate between sp^2- and sp^3- hybridization states (formal charge of -0.5 per atom). Ligand structures were relaxed via the default molecular mechanics optimization settings in SYBYL using the Tripos Force Field [14]. Low-barrier isomerisation of *O*-ribosyl-

substituents between the 2'- and 3'-oxygens in ribosyl-substituted nucleotides induces an uncertainty in the expected isomeric form of the docked ligand [10]. Accordingly, we initially considered both forms for each ligand. Ligand-receptor complexes were generated via flexible docking simulations using the FlexX program [15]. For each of the 12 MANT-nucleotides employed in the training set, 30 poses were requested, and all other parameters and convergence settings were left at default values. From the resulting complex manifold, a quantitative structure-activity relationship (QSAR) model was elaborated *via* the Comparative Binding Energy (COMBINE) method [16] for assessing specific interactions between the ligands and receptor residues. Weights for the specific interactions were trained from partial least squares (PLS) fitting to experimental K_i values (full-length EF structure in the presence of excess Mn^{2+}) via the SIMCA-P program [17].

2.5. Data analysis. All monophasic inhibition and saturation curves summarized in Table 1 were analyzed by non-linear regression using the Prism 4.0 software (Graphpad, San Diego, CA, USA). Fluorescence spectra were analyzed using the spectrum package of the Varian Cary Eclipse 1.1 software. For generation of graphs shown in Figs. 2 and 3, fluorescence data were imported into the Prism software.

3. Results

3.1. Inhibition of the catalytic activity of EF3 by MANT-nucleotides. Table 1 summarizes the K_i values of various MANT-adenine and MANT-guanine nucleotides for inhibition of the catalytic activity of EF3 in the presence of Mn^{2+} and in the presence of Mg^{2+}. Although Mg^{2+} is the physiologically relevant divalent cation, we also examined Mn^{2+} since with this cation, fluorescence and FRET signals are much larger than with Mg^{2+} [5]. In the presence of Mn^{2+}, racemic MANT-ATP and MANT-GTP were less potent EF3 inhibitors than

defined isomers. 3'-MANT-2'-deoxy-ATP was 4-fold more potent than 2'-MANT-3'-deoxy-ATP. Conversely, 2'-MANT-3'-deoxy-GTP was 7-fold more potent than 3'-MANT-2'-deoxy-GTP. In the presence of Mg^{2+}, inhibitor affinities were considerably lower than in the presence of Mn^{2+}. The potencies of 2'-MANT-3'-deoxy-ATP and 2'-MANT-3'-deoxy-GTP were particularly sensitive to the Mn^{2+}/Mg^{2+} exchange. Differential effects of Mg^{2+} and Mn^{2+} on MANT-nucleotide affinity were also observed for other nucleotides at EF and various nucleotides at mammalian ACs [5-9].

3.2. Direct fluorescence and FRET studies with EF3. Tryptophan (and tyrosine) residues are excited at λ_{ex} 280 nm [5,8,9], resulting in substantial endogenous fluorescence of EF3 with an emission maximum of λ_{em} 350 nm (Figs. 2A-2C and 3A-3C). At λ_{ex} 280 nm, MANT-nucleotides exhibited only minimal endogenous fluorescence, providing an excellent signal-to noise ratio for FRET studies. MANT-nucleotides show an increase in fluorescence upon an increase in hydrophobicity in the vicinity of the MANT-group [10,11]. Following the addition of CaM, with all MANT-nucleotides examined, new fluorescence peaks with a maximum of λ_{em} 425-430 nm became apparent. These new peaks reflect FRET from tryptophan and tyrosine residues to the MANT-group and were the result of the substantial CaM-induced conformational change in EF [2,5]. Interestingly, FRET with MANT-ATP and MANT-GTP was moderately smaller than with the corresponding 3'-MANT-isomers and much smaller than with the 2'-MANT-isomers. The FRET signal with 2'-MANT-3'-deoxy-GTP was particularly impressive. These differences in fluorescence were not due to endogenous differences in responsiveness to hydrophobic environments between nucleotides since a hydrophobic environment (30% (vol/vol) dimethyl sulfoxide) yielded similar relative fluorescence increases with the MANT-nucleotides studied (data not shown).

We also determined the K_d values of MANT-nucleotides by measuring peak CaM-stimulated FRET values and analyzing the data by non-linear regression (Table 1). Overall,

we found a good relation between the K_d values in the FRET assay and K_i values in the AC assay, the only exception being 3'MANT-2'-deoxy-ATP. This difference is probably due to the fact that the relatively high protein concentration used in the FRET assay underestimates the true affinity of this high-affinity ligand. It is noteworthy that the maximum FRET signals did not correlate with nucleotide affinity. Specifically, 3'-MANT-2'-deoxy-ATP exhibited a higher affinity than 2'-MANT-3'-deoxy-ATP in the AC- and FRET assay (Table 1), but the maximum FRET was much larger with 2'-MANT-3'-deoxy-ATP than with 3'-MANT-2'-deoxy-ATP (Figs. 2B and 2C).

In a classic FRET experiment, the appearance of the new emission peak at λ_{em} 425-430 nm should be accompanied by a corresponding decrease in the endogenous tryptophan- and tyrosine fluorescence peak at λ_{em} 350 nm [8,9,18]. However, for MANT-ATP, MANT-GTP, 3'-MANT-2'-deoxy-ATP and 3'-MANT-2'-deoxy-GTP, the appearance of the fluorescence peak at λ_{em} 425-430 nm was not accompanied by a decrease at λ_{em} 350 nm. Additionally, with 2'-MANT-3'-deoxy-ATP and 2'-MANT-3'-deoxy-GTP, the decrease in fluorescence at λ_{em} 350 nm was relatively small compared to the FRET peak. These findings are explained by a model in which part of the endogenous tryptophan and tyrosine fluorescence of EF3 is quenched by surrounding polar amino acids such as aspartate, glutamate and histidine [5,18]. Upon EF3 activation by CaM, a large conformational change in EF3 occurs [2,5], annihilating, to a large extent, the quenching effects of polar amino acids and masking the predicted decrease in fluorescence at λ_{em} 350 nm.

We also examined the direct MANT-nucleotide fluorescence by using an excitation wavelength of λ_{ex} 350 nm (Figs. 2D-2F and 3D-3F) [5,10,11]. At λ_{ex} 350 nm, MANT-nucleotides exhibited significant endogenous fluorescence with a maximum at λ_{em} 450 nm. The various MANT-nucleotides differed from each other in their endogenous fluorescence properties. However, as already stated above, the responsiveness of MANT-nucleotides to a

hydrophobic environment (dimethyl sulfoxide) was similar. The addition of EF3 to samples did not significantly change this basal fluorescence. However, upon addition of CaM, we observed clear increases in direct fluorescence with MANT-ATP, 2'-MANT-3'-deoxy-ATP, 3'-MANT-2'-deoxy-ATP and 2'-MANT-3'-deoxy-GTP, whereas with MANT-GTP and 3'-MANT-2'-deoxy-GTP, the fluorescence increases were minimal or absent. Increases in direct fluorescence were accompanied by decreases of the emission maximum by about 5 nm, referred to as blue-shift, reflecting transfer of the MANT-group into a more hydrophobic environment [5,11]. Previous studies have already shown that MANT-nucleotides are highly sensitive at detecting small differences in the interaction of ligands with the catalytic site of bacterial AC toxins including EF and mammalian AC [5,8,9,19].

3.3. Molecular modeling studies. Molecular docking studies predict that MANT-nucleotides are stabilized in the catalytic pocket of EF3 by Van der Waals and electrostatic interactions with several residues in EF3. The $NHCH_3$-group of MANT-ATP interacts with F586, E588 and N583 of EF3 (Fig. 4A). Amino acid residues T548 (above depicted plane and thus not shown) and T579 further enhance this interaction by stabilizing the base of the nucleotide. The anthraniloyl ring of the MANT-group is aligned in parallel to F586 and is stabilized by π-stacking interactions with F586. Those π-stacking interactions are important for direct MANT fluorescence signals (Figs. 2 and 3). Furthermore, the distances between the MANT-group and the tryptophan residues W357, W552, W608 and W645 in EF3 are predicted to be 16 Å, 22 Å, 14 Å and 17 Å respectively. This proximity between the tryptophan residues (donor) and the MANT-group (acceptor) explains the occurrence of FRET (Figs. 2 and 3) [18].

Molecular docking studies predict differential binding of the MANT-ATP and MANT-GTP isomers in the active site of EF3. Residues T548 and T579 may interact with the adenine base (Fig. 4A). This probably explains why MANT-ATP analogs are, in general, more potent

EF3 inhibitors than MANT-GTP analogs (Table 1). Additionally, in case of MANT-ATP analogs, the 3'-MANT isomer is better aligned with F586 than the 2'-MANT isomer to form π-stacking interactions (Fig. 4A), resulting in a higher affinity for EF3 in AC- and direct MANT fluorescence signals (Table 1). In contrast, the MANT-group of 3'-MANT-2'-deoxy-GTP is farther away from F586 than the MANT-group of 2'-MANT-3'-deoxy-GTP (Fig. 4B). This is also consistent with our experimental data indicating that the 2'-MANT isomer of MANT-GTP is more potent in AC- and FRET assays than the 3'-MANT isomer (Table 1).

The triphosphate chain of the MANT-nucleotides is stabilized by the interaction with residues R329, K346, K353, S354 and K372 of EF3 (Fig. 4). The γ-phosphate and the oxygen of the β-phosphate interact with R329, K353 and K372. The β-phosphate and the α,β-bridging oxygen is stabilized by interactions with S354 and K346. The β,γ-bridging oxygen is predicted to form hydrogen bonds with K353. As expected in the crystal structure of EF3 [2], the metal atoms are coordinated by H577, a pair of conserved residues, D491 and D493, and the non-bridging oxygens of the phosphate chain.

4. Discussion

Using enzymatic, fluorescence spectroscopy and molecular modelling approaches, our present study shows that the 2'- and 3'-isomers of MANT-ATP and MANT-GTP interact differentially with the catalytic site of EF. Thus, the results of this study lend further support to the broad hypothesis that the catalytic sites of various structurally unrelated ACs including mammalian membranous ACs and bacterial AC toxins exhibit substantial degrees of conformational flexibility, allowing for numerous structural modifications in nucleotide inhibitors and the development of AC isoform-selective inhibitors [5-9,19].

Our study demonstrates a remarkable dissociation between ligand-affinity for EF as assessed by inhibition of catalysis and FRET on one hand and both the maximum stimulation of direct fluorescence and FRET upon activation of CaM on the other hand. Most notably, 3'-MANT-2'-deoxy-ATP is the most potent EF3 inhibitor known so far (K_i, 10 nM), even surpassing the antiviral drug, adefovir (K_i, 27 nM) [4]. Nonetheless, in terms of maximum direct fluorescence and FRET signals, 3'-MANT-2'-deoxy-ATP is clearly surpassed by 2'-MANT-3'-deoxy-ATP and 2'-MANT-3'-deoxy-GTP (Figs. 2B and 3B). Similar dissociations between affinity and maximum fluorescence signals were observed for the comparison of MANT-ATP and MANT-CTP at EF [5]. An explanation for these discrepancies could be differences in mobility of the various fluorescence probes, with the more rigidly bound ligands being more effective in terms of direct MANT fluorescence and FRET [5,18].

Our data have important conceptual implications for future drug development. Specifically, for membranous mammalian ACs, a preference for the 3'-MANT isomer of MANT-ATP and MANT-GTP was observed using a crystallographic approach [8,9]. In contrast, for the first time, in this study we observed a preference of an AC for a 2'-MANT-isomer, specifically 2'-MANT-3'-deoxy-GTP (Table 1). However, this preference cannot be generalized since among MANT-ATP derivatives, EF showed higher affinity for the 3'-MANT isomer like in mammalian ACs [8,9]. Therefore, systematic synthesis and analysis of 2'- and 3'-*O*-ribosyl-substituted nucleotides may result in the development of potent EF inhibitors with high selectivity relative to mammalian membranous ACs. Considering than the fact that EF exhibits a uniquely high affinity for MANT-CTP [5], the analysis of 2'-MANT-3'-deoxy-CTP and 3'-MANT-2'-deoxy-CTP will be particularly interesting. However, such an analysis is not trivial since the starting material for the synthesis of 2'-MANT-3'-deoxy-CTP, 3'-deoxy-CTP, is not commercially available and has to be prepared *de novo*.

It will also be very interesting to examine the effects of carbamoyl-MANT-nucleotides on EF. In carbamoyl-substituted nucleotides isomerisation of the MANT-group between the

2'- and 3'-*O*-ribosyl group cannot take place. Stable carbamoylation may play an important role in the access of the inhibitor to the catalytic site. Moreover, a preserved 2'-OH- and 3'-OH group may allow for the formation of additional affinity-enhancing hydrogen bonds between EF and the ligand. An additional important issue for intact cell-studies is the membrane-permeability of nucleotides. The nucleotides studied herein do not cross the plasma membrane because they are too hydrophilic. One strategy to achieve membrane penetration is the pronucleotide approach. Specifically, in pronucleotides, a nucleoside 5'-monophosphate is protected at the phosphate group so that the nucleotide can cross the plasma membrane. Once inside the cell, the pronucleotide is deprotected and phosphorylated to the corresponding active nucleoside 5'-triphosphate [20].

Another important aspect that needs to be discussed is the fact that only in the presence of Mn^{2+}, but not in the presence of Mg^{2+}, 3'-MANT-2'deoxy-ATP and 2'-MANT-3'deoxy-GTP were 10-20-fold more potent than the corresponding racemic nucleotides. It is generally assumed that under neutral conditions, i.e. the assay conditions used in the present study, MANT-nucleotides exist as a racemic 1:1 mixture [10]. However, it is possible that the nature of the cation affects the isomerisation equilibrium. Such change in equilibrium could affect the access of the ligand to the catalytic site as well as the actual binding process. Conversely, the non-isomerising 3'-MANT-2'deoxy-ATP and 2'-MANT-3'deoxy-GTP may cause fewer steric clashes during the binding in the presence of Mn^{2+} than the corresponding isomerising nucleotides. However, currently, we cannot definitively answer this question. Given the fact that Mg^{2+} is the physiological cation, the isomer differences observed under Mg^{2+} conditions may be too small to be of relevance *in vivo*. The importance of studying MANT-nucleotides in the presence of Mg^{2+} has also been emphasized in a recent study on mouse heart AC [21].

Our present data have also practical implications for future EF inhibitor development. Specifically, the large CaM-dependent FRET signals with 2'-MANT-3'-deoxy-ATP (Fig. 2B)

and particularly with 2'-MANT-3'-deoxy-GTP (Fig. 3B) could be used as non-radioactive high-throughput screening assay for EF inhibitors, including compounds binding to the catalytic site as well as compounds impeding with the interaction of EF and CaM. The facts that the respective nucleotides are now commercially available and that EF can be readily purified in large amounts facilitate the establishment of a high-throughput screening assay. Such FRET assay constitutes a valuable complementation of the sensitive radiometric AC assay using [α-^{32}P]ATP as substrate and our recently developed non-radioactive terbium-norfloxacin assay, detecting PP_i [22].

To the best of our knowledge, this is the first study that systematically compares the interaction of two groups of MANT-nucleotides in their racemic form and as defined 2'- and 3'-isomers with a target protein. Using enzymological, biophysical and molecular modelling approaches, our data clearly show that each of the nucleotides studied interacts differently with EF. In support of our present study providing direct evidence, previous studies on various ACs and GTP-binding proteins using 2',3'-MANT-nucleotides and 3'-MANT-2'deoxy-nucleotides provided indirect evidence for differential interaction of target proteins with 2'-MANT- and 3'-MANT isomers [6,23,24].

Another property of defined 2'- and 3'-MANT isomers is that they differ from each other in their intrinsic fluorescence properties as is particularly evident for GTP derivatives (Figs. 3E and 3F). Accordingly, isomerisation of the MANT-group between the 2'- and 3'-position during the fluorescence experiment may superimpose the actual binding and hydrophobic interactions between the fluorophore and the target protein, potentially reducing fluorescence signals and rendering data interpretation difficult [23]. This notion is supported by the fact that with defined 2'-MANT isomers of ATP and GTP very large and robust fluorescence signals were obtained upon interaction with EF.

In conclusion, the results of our present study show that the systematic analysis of MANT-nucleotide racemates and defined 2'-MANT- and 3'-MANT isomers provides

valuable insights into the molecular mechanisms of ligand/enzyme interactions, yields highly sensitive fluorescence probes for protein analysis and facilitates the design of potent and selective enzyme inhibitors. In the past, such systematic studies could not be performed due to the non-availability of sufficient amounts of 3'-deoxy-GTP as starting material for synthesis [23]. Now, defined 2'- and 3'-MANT-isomers are commercially available at least for MANT-ATP and MANT-GTP.

Acknowledgements

We thank Drs. A. Gille and C. Pinto (Department of Pharmacology and Toxicology, University of Kansas) for helpful discussions and Dr. J. Geduhn (Institute of Organic Chemistry, University of Regensburg) for providing Fig. 1. Thanks are also due to the Reviewers for their most helpful suggestions and critique. This work was supported by Deutsche Forschungsgemeinschaft grant Se 529/5-1 to R. S. and NIH grant GM 062558 to W-.J. T.

References

[1] Jedrzejas MJ. The structure and function of novel proteins of *Bacillus anthracis* and other spore-forming bacteria: development of novel prophylactic and therapeutic agents. Crit Rev Biochem Mol Biol 2002;37:339-73.

[2] Drum CL, Yan SZ, Bard J, Shen YQ, Lu D, Soelaiman S, Grabarek Z, Bohm A, Tang WJ. Structural basis for the activation of anthrax adenylyl cyclase exotoxin by calmodulin. Nature 2002;415:396-402.

[3] Shen Y, Lee YS, Soelaiman S, Bergson P, Lu D, Chen A, Beckingham K, Grabarek Z, Mrksich M, Tang WJ. Physiological calcium concentrations regulate calmodulin binding and catalysis of adenylyl cyclase exotoxins. EMBO J 2002;21:6721-32.

[4] Shen Y, Zhukovskaya NL, Zimmer MI, Soelaiman S, Bergson P, Wang CR, Gibbs CS, Tang WJ. Selective inhibition of anthrax edema factor by adefovir, a drug for chronic hepatitis B virus infection. Proc Natl Acad Sci USA 2004;101:3242-7.

[5] Taha HM, Schmidt J, Göttle M, Suryanarayana S, Shen Y, Tang WJ, Gille A, Geduhn J, König B, Dove S, Seifert R. Molecular analysis of the interaction of anthrax adenylyl cyclase toxin, edema factor, with 2'(3')-*O*-(*N*-(methyl)anthraniloyl)-substituted purine and pyrimidine nucleotides. Mol Pharmacol 2009;75:693-703.

[6] Gille A, Lushington GH, Mou TC, Doughty MB, Johnson RA, Seifert R. Differential inhibition of adenylyl cyclase isoforms and soluble guanylyl cyclase by purine and pyrimidine nucleotides. J Biol Chem 2004;279:19955-69.

[7] Gille A, Seifert R. 2'(3')-*O*-(*N*-methylanthraniloyl)-substituted GTP analogs: a novel class of potent competitive adenylyl cyclase inhibitors. J Biol Chem 2003;278:12672-9.

[8] Mou TC, Gille A, Fancy DA, Seifert R, Sprang SR. Structural basis for the inhibition of mammalian membrane adenylyl cyclase by 2'(3')-*O*-(*N*-methylanthraniloyl)-guanosine 5'-triphosphate. J Biol Chem 2005;280:7253-61.

[9] Mou TC, Gille A, Suryanarayana S, Richter M, Seifert R, Sprang SR. Broad specificity of mammalian adenylyl cyclase for interaction with 2',3'-substituted purine- and pyrimidine nucleotide inhibitors. Mol Pharmacol 2006;70:878-86.

[10] Jameson DM, Eccleston JF. Fluorescent nucleotide analogs: synthesis and applications. Methods Enzymol 1997;278:363-90.

[11] Hiratsuka T. New ribose-modified fluorescent analogs of adenine and guanine nucleotides available as substrates for various enzymes. Biochim Biophys Acta 1983;742:496-508.

[12] SYBYL 7.2, The Tripos Associates, St. Louis, MO, USA, 2006.

[13] Gasteiger J, Marsili M. Iterative partial equalization of orbital electronegativity: a rapid access to atomic charges. Tetrahedron 1980;36:3219-28.

[14] Clark M, Cramer RD III; Van Opdenbosch N. Validation of the general purpose Tripos 5.2 force field. J Comput Chem 1989;10:982-1012.

[15] Rarey M, Kramer B, Lengauer T, Klebe GA. A fast flexible docking method using an incremental construction algorithm. J Mol Biol 1996;261:470-89.

[16] Ortiz AR, Pisabarro MT, Gago F, Wade RC. Prediction of drug binding affinities by comparative binding energy analysis. J Med Chem 1995;38:2681-91.

[17] SIMCA-P, Umereics AB: July, 2001.

[18] Lakowicz JR, *Principles of Fluorescence Spectroscopy*. Kluwer Academic/Plenum, New York, 1999.

[19] Göttle M, Dove S, Steindel P, Shen Y, Tang WJ, Geduhn J, König B, Seifert R. Molecular analysis of the interaction of *Bordetella pertussis* adenylyl cyclase with fluorescent nucleotides. Mol Pharmacol 2007;72:526-35.

[20] Laux WH, Pande P, Shoshani I, Gao J, Boudou-Vivet V, Gosselin G, Johnson RA. Pro-nucleotide inhibitors of adenylyl cyclases in intact cells. J Biol Chem 2004;279:13317-32.

[21] Göttle M, Geduhn J, König B, Gille A, Höcherl K, Seifert R. Characterization of mouse heart adenylyl cyclase. J Pharmacol Exp Ther 2009 (in press).

[22] Spangler CM, Spangler C, Göttle M, Shen Y, Tang WJ, Seifert R, Schäferling M. A fluorimetric assay for real-time monitoring of adenylyl cyclase activity based on terbium norfloxacin. Anal Biochem 2008;381:86-93.

[23] Rensland H, Lautwein A, Wittinghofer A, Goody RS. Is there a rate-limiting step before GTP cleavage by H-*ras* p21? Biochemistry 1991;30:11181-5.

[24] Moore KJM,Webb MR, Eccleston JF. Mechanism of GTP hydrolysis by $p21^{N\text{-}ras}$ catalyzed by GAP: studies with a fluorescent GTP analogue. Biochemistry 1993;32:7451-9.

Figure legends

Fig. 1. Structures of MANT-nucleotides. A, Structures of MANT-ATP, 3'-MANT-2'deoxy-ATP and 2'-MANT-3'-deoxy-ATP. **B**, Structures of MANT-GTP, 3'-MANT-2'deoxy-GTP and 2'-MANT-3'-deoxy-GTP. In MANT-ATP and MANT-GTP, the MANT-group is shown to be attached to the 3'-position, but spontaneous isomerisation can take place between the 2'- and 3'-*O*-ribosyl position. Under neutral pH conditions, i.e. the conditions used in this study, the 2'-and 3'-MANT isomers are in equilibrium. Due to the missing hydroxyl group in the 2'-deoxy- and 3'-deoxy derivatives, isomerisation of the MANT group in those compounds is impossible.

Fig. 2. Interaction of EF3 with MANT-adenine nucleotides in fluorescence experiments. Direct fluorescence studies and FRET studies were performed as described in Materials and Methods. Following the addition of various components (300 nM each) to fluorescence cuvettes, steady-state emission spectra were recorded. 1. Addition of MANT-adenine nucleotides (*solid* traces); 2. addition of EF3 (*dashed* traces); 3. addition of CaM (*dotted* traces). Panels **A-C** show representative FRET studies with an excitation wavelength λ_{ex} 280 nm; panels **D-E** show representative direct fluorescence studies with an excitation wavelength λ_{ex} 350 nm. Similar data were obtained in 5-6 experiments with different EF3 preparations.

Fig. 3. Interaction of EF3 with MANT-guanine nucleotides in fluorescence experiments. Direct fluorescence studies and FRET studies were performed as described in Materials and Methods. Following the addition of various components (300 nM each) to fluorescence cuvettes, steady-state emission spectra were recorded. 1. Addition of MANT-guanine nucleotides (*solid* traces); 2. addition of EF3 (*dashed* traces); 3. addition of CaM (*dotted* traces). Panels **A-C** show representative FRET studies with an excitation wavelength λ_{ex} 280 nm; panels **D-E** show representative direct fluorescence studies with an excitation wavelength λ_{ex} 350 nm. Similar data were obtained in 5-6 experiments with different EF3 preparations.

Fig. 4 Molecular modelling of the interactions of MANT-adenine- and guanine nucleotides. A, a superimposition of the 2'- and 3'-isomers of MANT-ATP in the space-filling model of EF3 is shown. Only important residues are rendered in the model, and the colors on the surface of EF3 are depicted as follows: Hydrophobic surfaces = *yellow*, acidic surfaces = *red*, basic regions = *blue*, neutral/polar = *white*. Ligands are depicted in stick form and are represented in the following colors: C = *gray for the 2'-isomer and brown for the 3'-isomer*, N = *dark blue*, O = *red*, P = *orange*. **B**, a plot of predicted 2'-MANT-3'-deoxy-GTP (stick with *green* C-atoms) and 3'-MANT-2'-deoxy-GTP (stick with *purple* C-atoms) binding conformers within the EF3 receptor is shown. Except for carbon atoms, all the other atoms are depicted as follows: H = *cyan*, N = *blue*, O = *red*, P = *orange*. The MANT-group of 2'-MANT-3'-deoxy-GTP faces towards F586, whereas in case of 3'-MANT-2'deoxy-GTP, MANT-group faces towards K353.

Table 1. Inhibition of the catalytic activity of EF3 by various MANT-nucleotides and affinities of MANT-nucleotides in FRET experiments

MANT-nucleotide	K_i AC assay with Mn^{2+} (μM)	K_d FRET assay with Mn^{2+} (μM)	K_i AC assay with Mg^{2+} (μM)
MANT-ATP	0.36 ± 0.03	0.19 ± 0.02	0.90 ± 0.07
2'-MANT-3'-deoxy-ATP	0.04 ± 0.01	0.11 ± 0.03	4.61 ± 0.20
3'-MANT-2'-deoxy-ATP	0.01 ± 0.002	0.07 ± 0.01	0.75 ± 0.04
MANT-GTP	1.08 ± 0.24	0.79 ± 0.30	8.82 ± 0.33
2'-MANT-3'-deoxy-GTP	0.05 ± 0.01	0.06 ± 0.02	4.35 ± 0.42
3'-MANT-2'-deoxy-GTP	0.36 ± 0.11	0.38 ± 0.03	9.92 ± 1.59

AC activity was determined as described under Materials and Methods in the presence of Mn^{2+} or Mg^{2+}. Reaction mixtures contained MANT-nucleotides at concentrations from 1 nM - 100 μM as appropriate to generate saturated inhibition curves. Inhibition curves were analyzed by non-linear regression and were best fitted to monophasic sigmoidal curves. K_i values were calculated from IC_{50} values using the previously determined K_m values [5,6]. Data shown are the means ± SD of 3-6 experiments performed in duplicates. FRET experiments were performed as described under Materials and Methods in the presence of Mn^{2+}. Reactions mixtures contained MANT-nucleotides from 10 nM - 1.3 μM. CaM-stimulated FRET was analyzed by non-linear regression and was best fitted to monophasic saturation curves. Data shown are the means ± SD of 3 independent experiments.

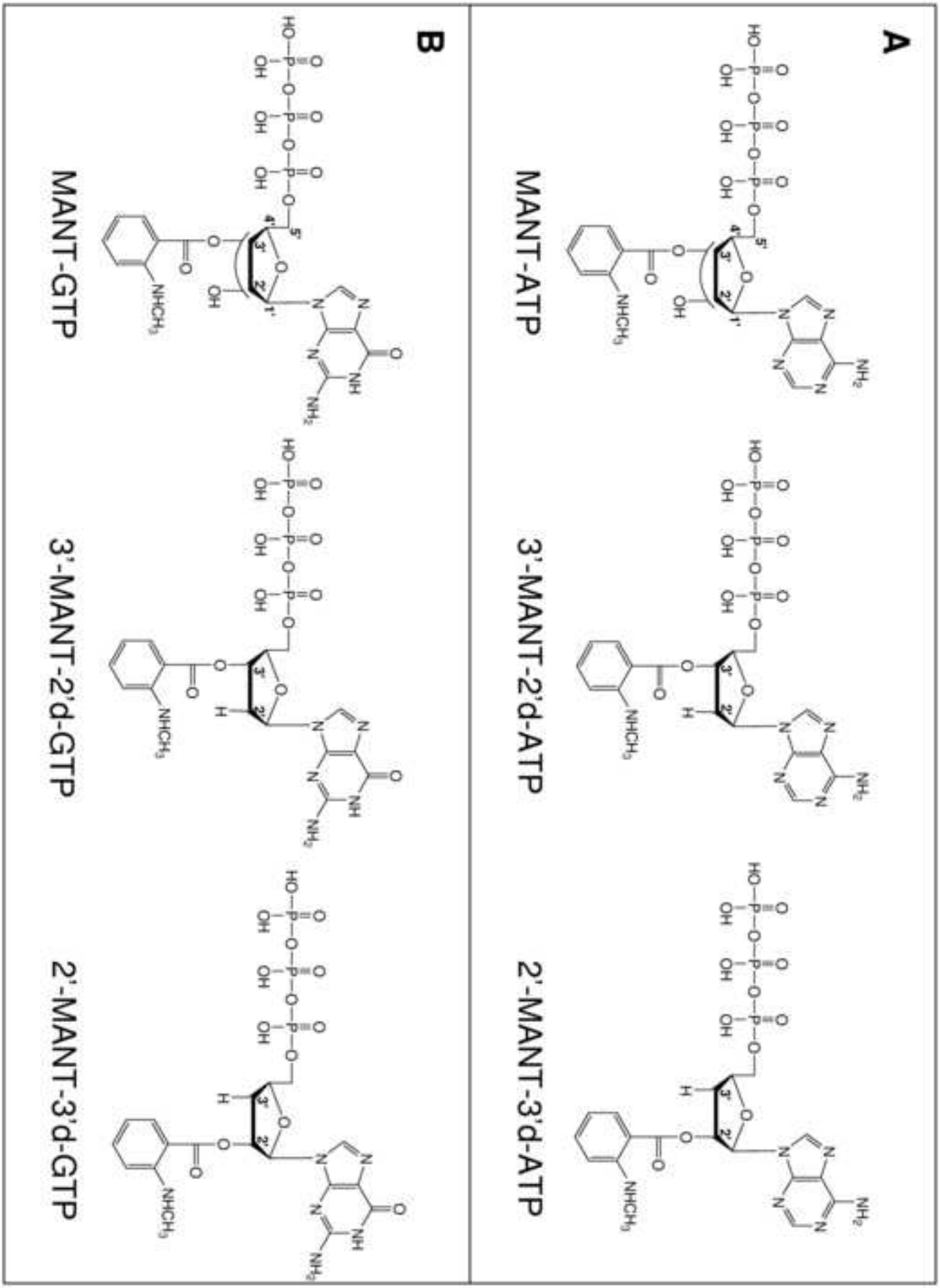

Figure 2

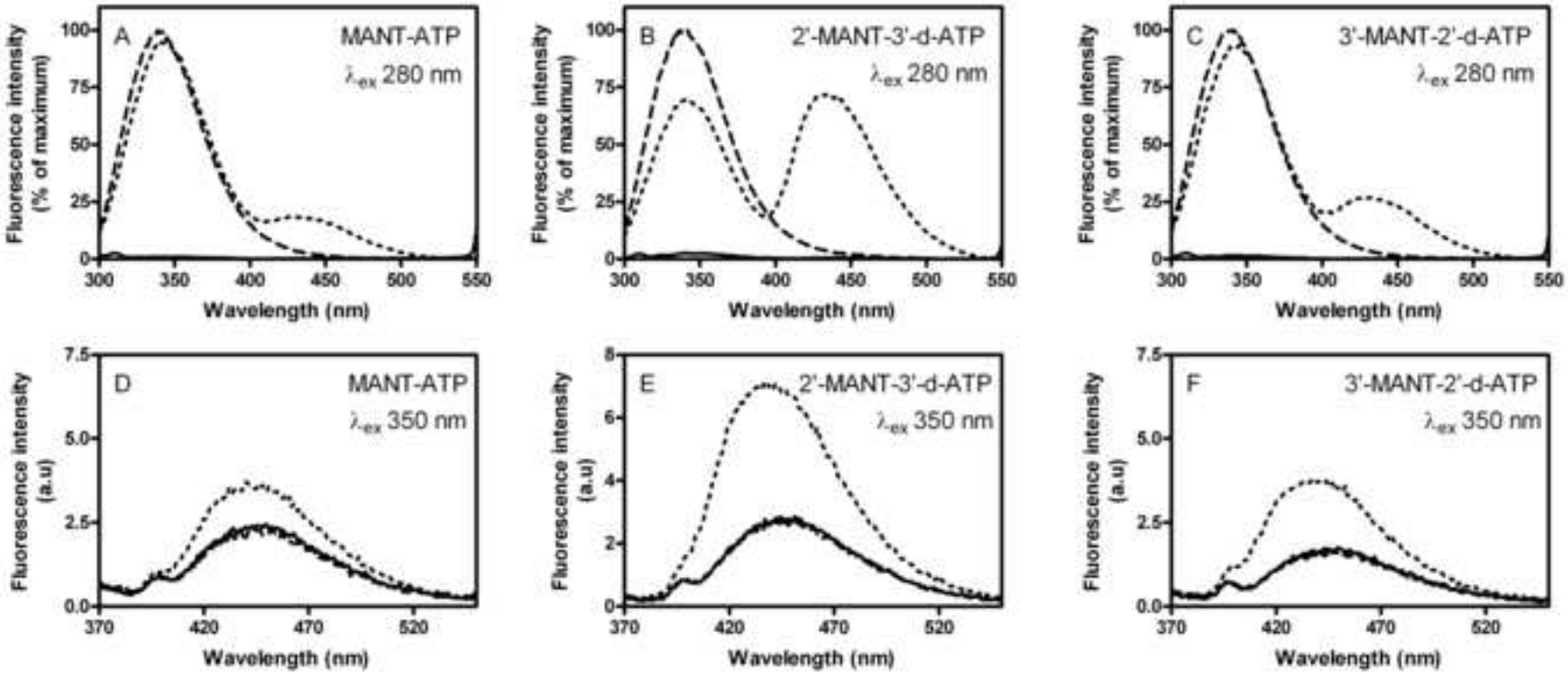
A
MANT-ATP
λex 280 nm
B
2'-MANT-3'-d-ATP
λex 280 nm
C
3'-MANT-2'-d-ATP
λex 280 nm
D
MANT-ATP
λex 350 nm
E
2'-MANT-3'-d-ATP
λex 350 nm
F
3'-MANT-2'-d-ATP
λex 350 nm
Fluorescence intensity (% of maximum)
Fluorescence intensity (a.u)
Wavelength (nm)

Figure 3

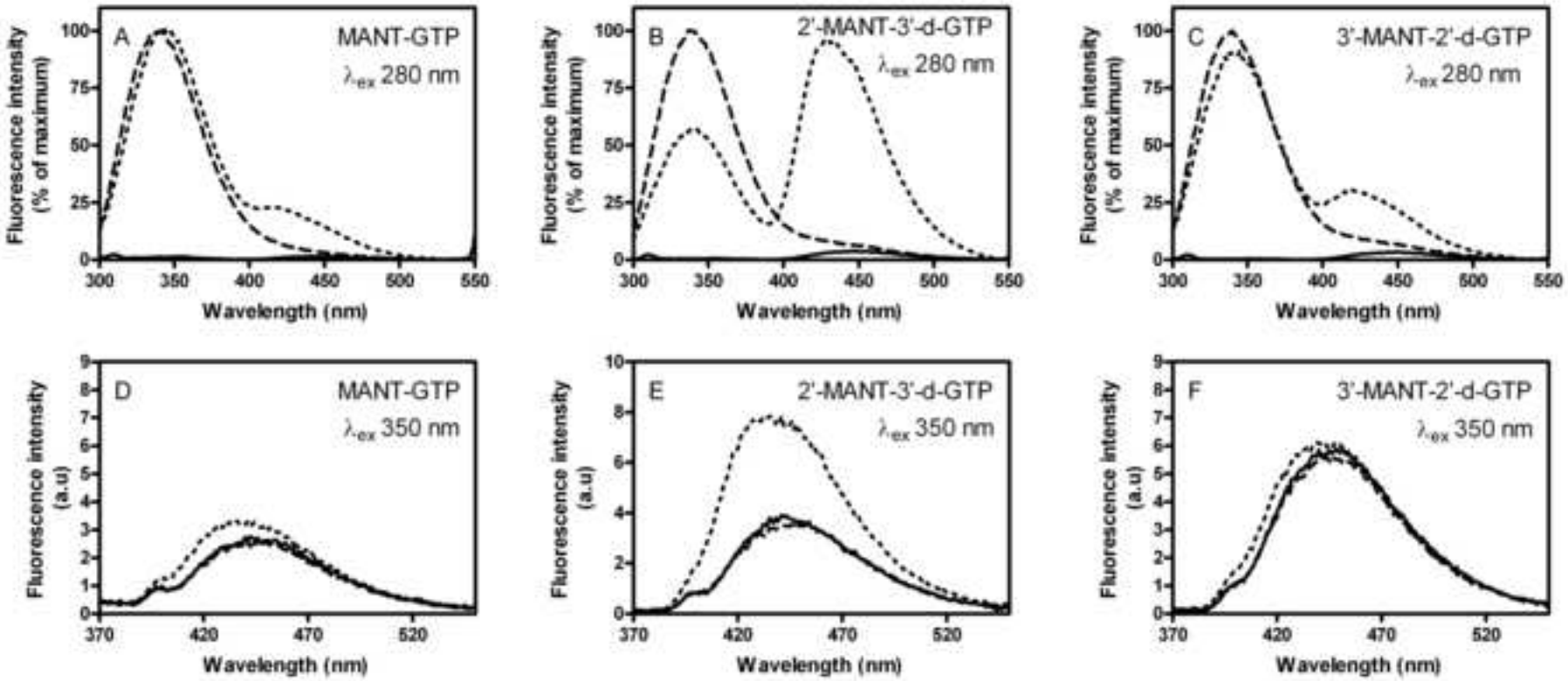
A
MANT-GTP
λex 280 nm
B
2'-MANT-3'-d-GTP
λex 280 nm
C
3'-MANT-2'-d-GTP
λex 280 nm
D
MANT-GTP
λex 350 nm
E
2'-MANT-3'-d-GTP
λex 350 nm
F
3'-MANT-2'-d-GTP
λex 350 nm
Fluorescence intensity (% of maximum)
Fluorescence intensity (a.u)
Wavelength (nm)